Activity dynamics in nonlocal interacting neural fields

Mihaela Enculescu and Michael Bestehorn
Lehrstuhl für Theoretische Physik II, Brandenburgische Technische Universität Cottbus, Erich-Weinert-Strasse 1, 03046 Cottbus, Germany
(Received 13 October 2002; revised manuscript received 8 January 2003; published 11 April 2003)

We study the activity of a synaptically coupled neuronal network consisting of an excitatory and an inhibitory layer with isotropic connections and nonlinear interactions. Using the mathematical model of Wilson and Cowan in two spatial dimensions, we first discuss a spatial hysteresis phenomenon. Then we analyze special traveling wave solutions with stationary shape. We establish existence conditions, derive analytic expressions of the particular solutions and their velocity, and finally present numerical simulations.

DOI: 10.1103/PhysRevE.67.041904 PACS number(s): 87.10.+e, 87.19.La, 87.18.−h

I. INTRODUCTION

Formation and propagation of excitation patterns in neural field models play an important role for understanding the information processing in the human brain (see Refs. [1–5]). Both experimental works and computational models of the brain show the occurrence of propagating patterns of activity in the thalamus and cortex neurons (e.g., Refs. [6–10]). Such waves can appear spontaneously or can be caused by some external stimulation.

Many authors analyzed cortical nervous tissues by means of mathematical field models, mostly derived by statistical considerations (see Ref. [11]). Solutions such as standing pulses and traveling fronts are intensively studied, providing the understanding of both naturally occuring and pathological phenomena [12–15].

In order to describe simple cortical and thalamic nervous tissues, Wilson and Cowan proposed in Ref. [16] an activator-inhibitor model based on few anatomically and physiologically motivated assumptions. They derived a mathematical system of integro-differential equations for the time-course grained firing rates of the excitatory and inhibitory neurons.

In the following section, we present the neural field model proposed by Wilson and Cowan. Then we extend the spatial hysteresis discussed in Ref. [16] to the case of two spatial dimensions. In Sec. IV we study traveling wave solutions with stationary shape. Although not in the basic equations included, the rotational symmetry seems to be characteristic for such waves in two spatial dimensions. For the case of a wave profile which is macroscopic compared with the range of the synaptical coupling, the velocity, shape, and the existence conditions of such solutions can be established analytically.

II. FIELD EQUATIONS

Let $E(\vec{r},t)$ and $I(\vec{r},t)$ denote the time-course grained firing rates of the excitatory and inhibitory neurons located at the place $\vec{r}=(x,y)$ at time t. Furthermore, let $P(\vec{r},t)$ be the external excitation on the activator field at $\vec{r}$. The equations proposed by Wilson and Cowan read

$$\frac{\partial E}{\partial t} = -E + S_E[w_{EE} * E - w_{EI} * I + P],$$

$$\frac{\partial I}{\partial t} = -I + S_I[w_{IE} * E - w_{II} * I]. \tag{1}$$

The output functions $S_E[x]$ and $S_I[x]$ are nonlinear, monotonic, nonincreasing, and saturate for values of x. In this paper, we consider the special case where the output function is the step function, namely,

$$S_k[x] = \begin{cases} 0, & x < V_k, \\ & \quad , \quad k \in \{E,I\}. \\ 1, & x \geqslant V_k, \end{cases} \tag{2}$$

Thus, a neuron fires at its maximum rate if the potential exceedes a threshold, otherwise it does not fire.

By $w*F$, we denote the linear convolution:

$$w*F(\vec{r},t) = \int_{\mathbb{R}^2} w(\vec{r}-\vec{r}')F(\vec{r}',t)d\vec{r}'. \tag{3}$$

The kernels $w_{EE}(\vec{r}), \ldots, w_{II}(\vec{r})$ are monotonically decreasing functions of the distance $r := |\vec{r}|$ between interacting neurons. We consider the normalized functions

$$w_{ik}(\vec{r}) = \frac{a_{ik}}{2\pi\sigma_{ik}^2} \exp\left(-\frac{r}{\sigma_{ik}}\right), \quad i,k \in \{E,I\}. \tag{4}$$

This means that the coupling between both excitatory and inhibitory cells is isotropic and homogeneous in space and time. The homogeneous approximation of the spatial network, assumed in this paper, may play a deciding role for the wave propagation. Recently, Bresloff showed for a related mathematical model that a propagation failure can occur in an inhomogeneous neural network, if the degree of inhomogeneity is too large, or the speed is too slow [17].

III. SPATIAL HYSTERESIS

As referred by Wilson and Cowan in Ref. [16], the model equations (1) might explain the spatial hysteresis observed in the binocular vision like in the Fender-Julesz experiment

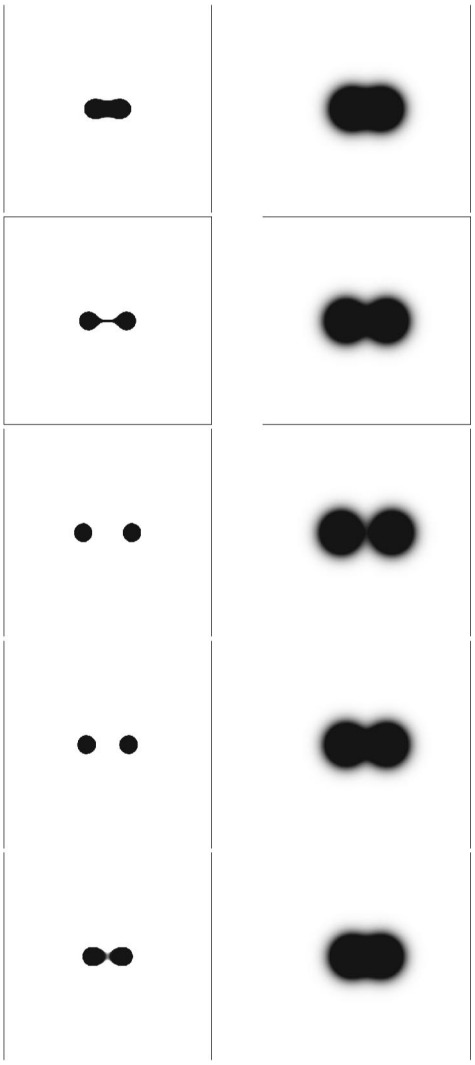

FIG. 1. Evolution of the excitatory field (left) in the presence of a time-dependent stimulation field (right) for $a_{EE}=20$, $a_{EI}=10.1$, $a_{IE}=4$, $a_{II}=1$, $V_E=10$, $V_I=2$, $p=11$. The position of the stimuli are identical in pictures 1 and 5, and in pictures 2 and 5, respectively.

[18]. Wilson and Cowan made the following numerical experiment with the corresponding one-dimensional–tissue model of Eq. (1): the stimulation $P(x,t)$ consists of a pair of sharply peaked Gaussian distributions equal in amplitude and shape. These are initiatially overlapped, so that the neural response consists of a single excitated area. The two stimuli are then symmetrically moved apart. The velocity of the stimuli is thereby small enough such that the neural response is allowed to reach equilibrium for every distance between the stimuli. For a critical stimulus disparity, the neural response splits into two separated peaks. The distance between the response peaks will increase with further increasing of the stimulus disparity. If the stimuli are then again moved together, the neural response peaks will fuse for a critical disparity of the stimuli. However, this critical disparity is much less than the first critical distance.

The representation (Fig. 1) shows the results of the numerical simulation corresponding to the two-dimensional tissue. The stimulus field $P(\vec{r},t)$ is given by

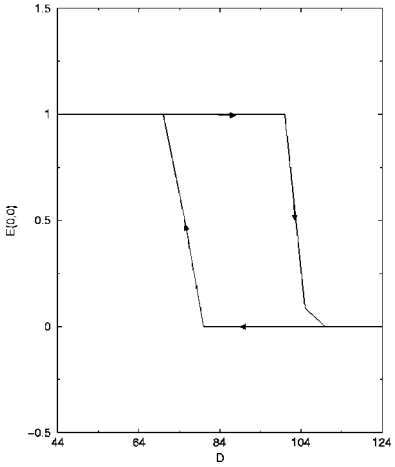

FIG. 2. Excitatory field in the middle of the square as a function of the distance between the stimulation peaks for the representation of Fig. 1.

$$P(\vec{r},t)=\frac{p}{2}\left\{\exp\left[-\frac{(x-vt)^2+y^2}{\sigma^2}\right]+\exp\left[-\frac{(x+vt)^2+y^2}{\sigma^2}\right]\right\}. \tag{5}$$

There are 512×512 discretization points. The convolution kernels have the same width equal to four discretization points. The width σ of the Gaussian peaks in Eq. (5) measures 40 points. The distance between the stimuli is varied in steps. For every position of the stimuli, the system is allowed to reach equilibrium. In the first picture of Fig. 1, there is only one excitated area in the neural response. The second picture (vertically numbered) shows the moment before the pattern in the neural response switches into two separated peaks. In the next picture, the sign of the velocity v is changed. The critical disparity of the stimuli, necessary to cause fusion of the peaks in the neural response (fourth picture), is less than the one required for the separation. The value of the excitatory field in the middle of the square is represented in Fig. 2 as a function of the stimulus disparity, showing a hysteresis loop.

In the following, we give an explanation of this hysteresis in the special case, where the stimuli peaks are macroscopic in relation to the typical interaction lenghts between neurons. If the space constant σ of the stimulus field P is very large as compared to the neural interaction ranges σ_{EE}, . . . , then at the point $\vec{r}_0$ the solution of the field corresponds to a homogeneous solution of the system which is stimulated by a homogeneuos field of amplitude $P(\vec{r}_0,t)=:P_0$. If the system is allowed to reach a stationary solution for every position of the stimuli peaks, then $E(\vec{r}_0,t)$ and $I(\vec{r}_0,t)$ are solutions of

$$E=S_E(a_{EE}E-a_{EI}I+P_0),$$

$$I=S_I(a_{IE}E-a_{II}I). \tag{6}$$

Excluding the improbable case $a_{IE}<V_I$, that is the inhibitor field is always zero, the system (6) can have the following solutions (E,I):

$$(1,1) \text{ if } \begin{cases} P_0>V_E+a_{EI}-a_{EE} & \text{(I)} \\ a_{IE}>a_{II}+V_I & \text{(II)}; \end{cases}$$

$$(0,0) \text{ if } P_0<V_E \text{ (III)}.$$

If the parameters of the system fulfill the condition (II) and if $a_{EI}<a_{EE}$ holds true, then the solutions of Eq. (6) read the following:

$$(0,0) \text{ for } P_0<V_E-(a_{EE}-a_{EI})=:P_1,$$

$$(0,0) \text{ and } (1,1) \text{ for } V_E-(a_{EE}-a_{EI})<P_0<V_E=:P_2,$$

$$(1,1) \text{ for } P_0>V_E.$$

Thus, for very small as well as for very large amplitudes of the stimuli, there exists only one stationary solution: $(0,0)$ and $(1,1)$, respectively. However, for

$$P_0\in[V_E-(a_{EE}-a_{EI}),V_E],$$

the system can choose between the resting state and the excitated solution. If we start with the unstimulated system and increase the amplitude of the stimulation, the solution will switch from the resting state into the excitated state for $P_0=P_2$. Once the system reaches the excitated state, it will stay there even if the stimulation decreases below P_2: the solution switches to the resting state only at $P_0=P_1<P_2$.

Let us apply these results to the numerical simulation of Fig. 1, for which

$$0<a_{EE}-a_{EI}<V_E$$

holds true. The amplitude of the stimulus at the center of the square $(x,y)=(0,0)$ is given by

$$P_0(D)=p\exp\left(-\frac{D^2}{4\sigma^2}\right),$$

where $D>0$ is the stimulus peak disparity. Starting with the excited state at $P_0(0)=p$ and increasing the stimulus disparity D will cause the separation of the neural response into two peaks at the critical disparity

$$D_1=2\sigma\sqrt{\ln\left(\frac{p}{P_1}\right)}=2\sigma\sqrt{\ln\left(\frac{p}{V_E-a_{EE}+a_{EI}}\right)}.$$

If the sign of v is changed, and the two stimulation peaks are moved together, the peaks in the neural response will fuse again at the critical disparity

$$D_2=2\sigma\sqrt{\ln\left(\frac{p}{P_2}\right)}=2\sigma\sqrt{\ln\left(\frac{p}{V_E}\right)},$$

which is smaller than D_1.

IV. STATIONARY WAVE FRONTS

In this section, we study the propagation of excitation fronts that arise for an inhomogeneuos external stimulation of the activator $P(\vec{r},t)$. Let the excitatory field be stimulated inside a narrow area around $\vec{r}=0$ by the constant external field $P_0(\vec{r})$ given by

$$P(\vec{r},t)=P_0(\vec{r})=\begin{cases} P, & \vec{r}=0 \\ 0, & \vec{r}\neq 0. \end{cases} \tag{7}$$

Due to the term P, the excitatory field E and also the inhibitory field I triggered by that will start to grow at $\vec{r}=0$. Numerical simulations show for this case two different solution types. In the first case, only neurons in the vicinity of the stimulated point will be excited, but this excitation does not spread out. There may appear stationary solutions, but also localized oscillations, depending on the choosen parameters of the problem. In the second case, the oscillation at $\vec{r}=0$ spreads out and propagates in the form of concentrical rings. We study this last solution type in the following.

Motivated by the special form of the numerical solutions of Eq. (1), we search for traveling patterns of excitation with stationary shape and velocity, this means solutions of the form

$$E(\vec{r},t)=g_1(r-vt),$$

$$I(\vec{r},t)=g_2(r-vt). \tag{8}$$

Due to the convolution terms, Eqs. (1) are not invariant under the tranformation $r\mapsto r-vt$. Thus, a global solution will not have the form expressed by Eqs. (8). However, far enough from the center of the excitation, namely, for

$$r\gg\sigma_{ik},i,k\in\{E,I\}, \tag{9}$$

the convolution terms such as $w*E(\vec{r},t)$ can also be written in form (8). In fact, taking Eq. (9) into account, we can approximate this convolution terms as follows:

$$w*E(\vec{r},t)=\int_0^\infty\int_0^{2\pi}w(r')g_1(r-vt+r'\cos\varphi)r'dr'd\varphi. \tag{10}$$

Thus, there may exist solutions of Eq. (1) which have form (8) for large values of r. Setting

$$z:=r-vt, \tag{11}$$

we get for the $g_1(z)$ and $g_2(z)$ the system

$$-vg_1'(z)=-g_1+S_E[w_{EE}*g_1-w_{EI}*g_2],$$

$$-vg_2'(z)=-g_2+S_I[w_{IE}*g_1-w_{II}*g_2]. \tag{12}$$

Since $r=0$ is the center of the wave and v its velocity, the fields E and I should be unperturbated for $r>vt$. Therefore, we have the boundary conditions

$$g_1(0)=g_2(0)=0. \tag{13}$$

Solving Eqs. (12) yields the stationary shape of the excitation waves for the two types of neurons. To this end, we analyze the sign of the expressions

$$G_1(z):=w_{EE}*g_1-w_{EI}*g_2-V_E \text{ and}$$

$$G_2(z):=w_{IE}*g_1-w_{II}*g_2-V_I. \tag{14}$$

The simplest possible form of the wave is that with one maximum, this means that each of g_1 and g_2 are monotonically decreasing only in one bounded interval. Let $(a,0)$ and (c,b), where $a<0$, $c<b$, denote the intervals where g_1 and g_2 are monotonically decreasing functions of z. There follows:

$$G_1(z)=\begin{cases} >0, & z\in(a,0) \\ <0, & \text{otherwise;} \end{cases}$$

$$G_2(z)=\begin{cases} >0, & z\in(b,c) \\ <0, & \text{otherwise.} \end{cases} \tag{15}$$

The solution of Eqs. (12) then takes the form

$$g_1(z)=\begin{cases} 0, & z>0 \\ 1-\exp\left(\dfrac{z}{v}\right), & a<z<0 \\ \left[\exp\left(-\dfrac{a}{v}\right)-1\right]\exp\left(\dfrac{z}{v}\right), & z<a; \end{cases}$$

$$g_2(z)=\begin{cases} 0, & z>b \\ 1-\exp\left(\dfrac{z-b}{v}\right), & c<z<b \\ \left[\exp\left(-\dfrac{c}{v}\right)-\exp\left(-\dfrac{b}{v}\right)\right]\exp\left(\dfrac{z}{v}\right), & z<c. \end{cases} \tag{16}$$

From Eqs. (14), we see that G_2 can only be positive at a certain point z, if g_1 is positive at this point. Since $g_1(z)=0$ for $z>0$, we then have $c<b<0$. The excitation can only propagate in this form if the wave of the activator is traveling in front of the inhibitor wave. Furthermore, it follows from Eqs. (15) and (16) that G_1 is increasing and g_1 decreasing with z for $z\to a$, $z>a$. This is only possible if g_2 is a decreasing function of z at this point, which means $c<a<b$. Thus, we have

$$c<a<b<0. \tag{17}$$

The velocity v and the parameters a,b,c can be determined by inserting the solutions g_1 and g_2 in Eqs. (14) and solving the four conditions

$$G_1(0)=G_1(a)=0,$$

$$G_2(b)=G_2(c)=0. \tag{18}$$

We do this under the approximation that the dimensions of the wave are very large compared with the ranges of the interaction, that is,

$$\sigma_{ik}\ll v,-b,b-a,a-c, \quad i,k\in\{E,I\}. \tag{19}$$

In this case, the expression $G_1(0)$ simplifies to (see the Appendix)

$$G_1(0)\approx\frac{2a_{EE}\sigma_{EE}}{\pi v}-V_E. \tag{20}$$

We obtain the velocity of the wave

$$v=\frac{2a_{EE}\sigma_{EE}}{\pi V_E}. \tag{21}$$

We have further

$$G_2(b)\approx a_{IE}\left[1-\exp\left(\frac{b}{v}\right)\right]-\frac{2a_{II}\sigma_{II}}{\pi v}-V_I \tag{22}$$

and condition (18) yields

$$b=-v\ln\left(\frac{a_{IE}}{a_{IE}-V_I-V_E\dfrac{a_{II}\sigma_{II}}{a_{EE}\sigma_{EE}}}\right). \tag{23}$$

We determine the parameter a from

$$G_1(a)\approx a_{EE}\left[1-\exp\left(\frac{a}{v}\right)\right]-\frac{2a_{EE}\sigma_{EE}}{\pi v} -a_{EI}\left[1-\exp\left(\frac{a-b}{v}\right)\right]-V_E, \tag{24}$$

and we get

$$a=-v\ln\left[\frac{a_{EI}\exp\left(-\dfrac{b}{v}\right)-a_{EE}}{a_{EI}-a_{EE}+2V_E}\right]. \tag{25}$$

Finally, the last parameter c results from the condition $G_2(c)=0$. Using the approximation (19), we have

$$G_2(c)\approx a_{IE}\exp\left(\frac{c}{v}\right)\left[\exp\left(-\frac{a}{v}\right)-1\right] -a_{II}\left[1-\exp\left(\frac{c-b}{v}\right)\right]-V_I \tag{26}$$

and the parameter c results to be

$$c=-v\ln\left\{\frac{a_{IE}\left[\exp\left(-\dfrac{a}{v}\right)-1\right]+a_{II}\exp\left(-\dfrac{b}{v}\right)}{V_I+a_{II}}\right\}. \tag{27}$$

Verifying the inequalities (17), we gain the conditions that should be filled out by the parameters of the system in order

for such a wave to propagate. The solution for v,a,b,c should also be consistent with approximation (19).

For the sake of simplicity, we neglect the self-inhibition of the inhibitor neurons by taking $a_{II}=0$. This does not change the following computation much but simplifies the results and their interpretation. From $b<0$, we see the condition

$$a_{IE}>V_I. \tag{28}$$

The condition $a<b$ leads to the inequalities

$$a_{EE}>2V_E\frac{a_{IE}}{V_I} \quad \text{and}$$

$$a_{EI}>a_{EE}-2V_E. \tag{29}$$

With this choice of the parameters, the last condition $c<a$ is automatically fulfilled. Due to

$$\exp\left(-\frac{b}{v}\right)<\exp\left(-\frac{a}{v}\right), \tag{30}$$

we have

$$(a_{IE}-V_I)\exp\left(-\frac{a}{v}\right)>a_{IE} \tag{31}$$

and further

$$\frac{a_{IE}\left[\exp\left(-\frac{a}{v}\right)-1\right]}{V_I}>\exp\left(-\frac{a}{v}\right). \tag{32}$$

In conclusion, a traveling wave of form (16) will exist if the choosen parameters of the system (with $a_{II}=0$) satisfy the conditions

$$a_{IE}>V_I,$$

$$a_{EE}>2V_E\frac{a_{IE}}{V_I}, \quad \text{and}$$

$$a_{EI}>a_{EE}-2V_E. \tag{33}$$

The first two inequalities show that the activator action on the inhibitor and activator must be greater than a factor proportional with the thresholds V_I and V_E. This conditions probably ensure the point to point propagation of the excitation in the activator and inhibitor fields. The interpretation of the third condition is that the inhibition of the activator must be greater than the self-activation. This is a very important condition, ensuring that those points that are excitated by the activator wave return into the resting state when the inhibitor wave arrives. In consequence, each point will have a refractory period after the excitation wave has passed. The points behind the excitation front of the activator are then inhibited and also act like a barrier for every excitation front traveling in the opposite direction. Thus, rings coming from different excitation centers will vanish when they meet. These results apply to the case where approximation (19) is correct. From $v\gg\sigma_{EE}$, it follows in particular that the coefficient a_{EE} of the self-activation should be much larger than the threshold V_E.

Finally, we can determine the distance between two successively released rings λ from the condition

$$w_{EE}*g_1(-\lambda)-w_{EI}*g_2(-\lambda)+P=V_E. \tag{34}$$

Following approximation (19), we obtain

$$\lambda=v\ln\left[\frac{a_{EI}(e^{-c/v}-e^{-b/v})-a_{EE}(e^{-a/v}-1)}{P-V_E}\right]. \tag{35}$$

We finally present numerical results for system (1) with an external stimulation P of form (7). The parameters of the system respect the restrictions above mentioned . There are 512×512 discretization points. The convolution kernels have the same width σ, and the distance between two discretization points is $\sigma/3.2$.

In the first representation (Fig. 3), there is only one stimulated area (3×3 points) in the middle of the field. Concentrical rings of excitation are periodically released and are propagating without attenuation. One can clearly see the delay in the propagation of the two excitation fronts of the activator and inhibitor cells that we discussed in the preceding section.

In order to have evidence for the interaction of different waves, there are two separated stimulated areas in the second representation (Fig. 4). Each of them gives rise to a system of concentrical rings. This numerical simulation shows the remarkable property of mutual annihilation upon collision of traveling waves.

The properties revealed by these simulations remind very much of the traveling waves of activity in the so-called ''excitable media,'' as in the Belousov-Zhabotinskii reaction, or the spread of a forest fire. Like these systems, our network has the ability to propagate signals without damping, and as characteristic to excitable media, two signals started from different sources cancel when they collide.

In signals coming from biological systems, there is always a lot of noise. Therefore, we discuss in the following the impact of noise on the traveling wave solution. To this end, we analyze the behavior of the system when it is stimulated by the external field

$$P(\vec{r},t)=P_0(\vec{r})+p(\vec{r}),$$

where P_0 is the unperturbated field (7), and $p(\vec{r})$ a small perturbation with spatial uniformly distributed amplitude. Therefore,

$$\langle p(\vec{r})\rangle=0$$

holds true. The numerical simulation of Fig. 5 shows for this case a perturbated traveling wave solution with qualitatively the same form as for the unperturbated system. Beside the defects in the form of the wave front, there is an important difference in the propagation speed, and the distance between two successive wave fronts. Several numerical simu-

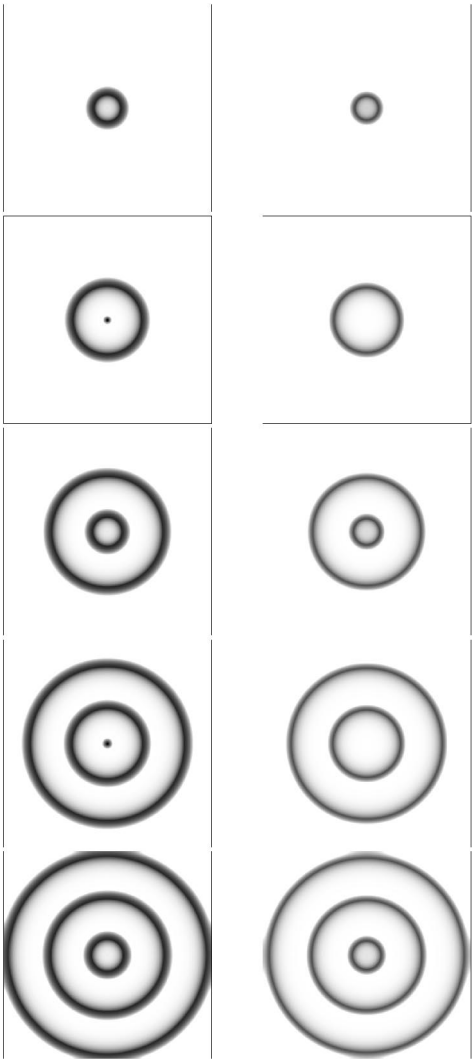

FIG. 3. Time evolution of the activator (left) and inhibitor field (right) for $a_{EE}=8.3$, $a_{EI}=10$, $a_{IE}=4$, $a_{II}=0$, $V_E=1$, $V_I=2.4$. A small area in the middle of the square is stimulated by the constant stimulation $P=1.2$.

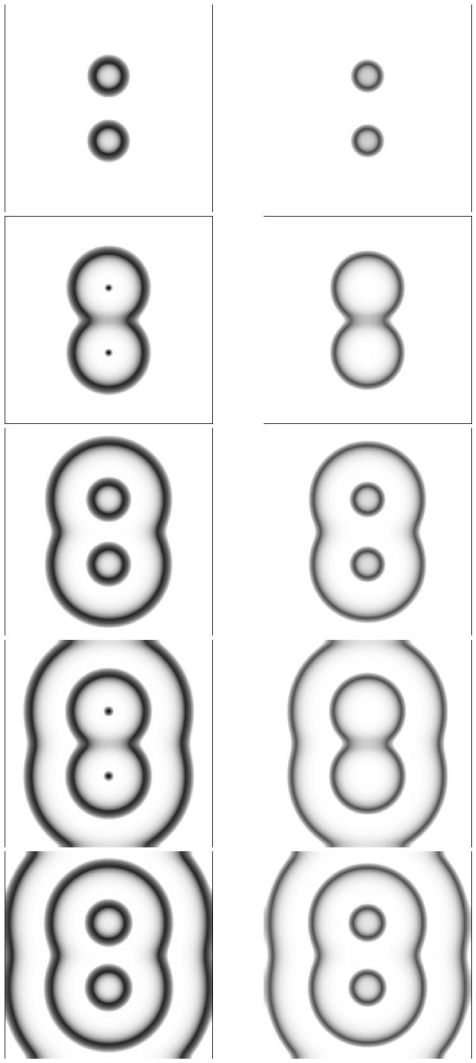

FIG. 4. Time evolution of the activator (left) and inhibitor field (right) for the same set of parameters as in (Fig. 3) and two symmetrically positioned stimulation centers.

lations with noise have actually shown, that the wave propagates faster that in the unperturbated case, and with larger wavelength.

V. DISCUSSION

In the first part of this paper, we analyzed a spatial hysteresis phenomenon for the two-dimensional neural field model of Wilson and Cowan. Hysteresis occurs only if the ratio

$$\frac{a_{EE}-a_{EI}}{V_E} \tag{36}$$

takes values in the interval (0,1) and if the amplitude of the stimulus is large enough ($p>V_E$). The size of the hysteresis loop seems to be proportional to the ratio (36), so this phenomen accentuates for

$$V_E-a_{EE}+a_{EI}\to+0.$$

In the second part, we studied traveling wave solutions of system (1) in the presence of a localized stimulation. Under certain conditions, rings of excitation will propagate from the stimulated point. Far enough from the center of stimulation, the excitation travels with constant velocity and amplitude. It is remarkable that the propagation speed of the wave depends only on the parameters concerning the self-activation of the system: In approximation (19), the calculated velocity is growing with the strength and the range of the activator-activator interaction and it is in inverse proportion to the threshold V_E.

Our results have revealed the importance of the inhibitory connections for the existence of the traveling wave solution. There always exists a time delay between the activation wave of the excitatory and inhibitory neurons, which plays a decisive role for the wave propagation. A similar mechanism was reported for slow pulse propagation in one-dimensional

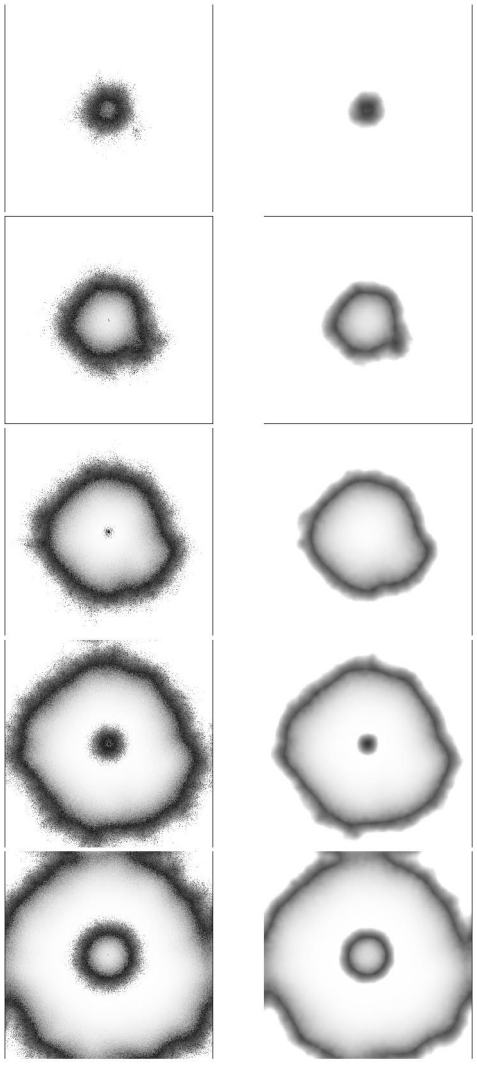

FIG. 5. Time evolution of the activator (left) and inhibitor field (right) for the same set of parameters as in (Fig. 3) and with uniformly distributed noise. The interval of time between two successive pictures is half of the similar time of Fig. 3.

networks of excitatory and inhibitory integrate and fire neurons by Golomb and Ermentrout (see Refs. [14,15]).

As in Ref. [10], we found that the wave front velocity increases linearly with the characteristic length of the connectivity σ_{EE}. By contrast, the propagation speed in our approximation depends linearly on the synaptic strength a_{EE}, and not logarithmically, as in Ref. [10].

The amplitude of the stimulation P does not influence this propagation speed, but rather the distance between two successively released rings.

APPENDIX

In this section, we describe the approximations used in the evaluation of Eqs. (20), (24), (22), and (26).

In order to compute $G_1(0), G_1(a), \ldots$, we need the convolutions $w_{EE}*g_1$, $w_{EI}*g_2, \ldots$ at the evaluation points $0,a, \ldots$. Due to the form of the interaction kernels $w_{EE}, \ldots$, only the points in the vicinity of radius $\sigma_{EE}, \ldots$ have a significant contribution to the corresponding convolution integrals. Thereby, if the dimensions of the wave are very large compared with the range of the interaction kernels $\sigma_{EE}, \ldots$, we just have to consider the solution parts of g_1 and g_2 immediately on the left and on the right side of the point, where the convolution has to be calculated.

For example, to evaluate $G_1(0)$ we need the convolutions $w_{EE}*g_1(0)$ and $w_{EI}*g_2(0)$. Due to $g_1(z)=0$ if $z>0$, we have

$$\begin{aligned} w_{EE}*g_1(0) &= \int_0^{\infty}\int_0^{2\pi} \frac{a_{EE}}{2\pi\sigma_{EE}^2}\exp\left(-\frac{\rho}{\sigma_{EE}}\right) \\ &\quad \times g_1(\rho\cos\varphi)\rho\, d\rho\, d\varphi \\ &= \int_0^{\infty}\int_{\pi/2}^{3\pi/2} \frac{a_{EE}}{2\pi\sigma_{EE}^2}\exp\left(-\frac{\rho}{\sigma_{EE}}\right) \\ &\quad \times g_1(\rho\cos\varphi)\rho d\rho d\varphi. \end{aligned} \tag{A1}$$

For large values of a compared with the range of the interaction kernels w_{EE}, only the values of g_1 in the close vicinity of the point 0, where the convolution is calculated, have a contribution to this integral. Thus, with approximation (19) we can substitute in the integral (A1) the solution g_1 for $a<z<0$

$$\begin{aligned} w_{EE}*g_1(0) &\approx \int_0^{\infty}\int_{\pi/2}^{3\pi/2} \frac{a_{EE}}{2\pi\sigma_{EE}^2}\exp\left(-\frac{\rho}{\sigma_{EE}}\right) \\ &\quad \times [1-e^{\rho\cos\varphi/v}]\rho d\rho d\varphi \\ &= \pi a_{EE}\sigma_{EE}^2 - a_{EE}\int_{\pi/2}^{3\pi/2} \frac{d\varphi}{\left(-\frac{1}{\sigma}+\frac{\cos\varphi}{v}\right)^2}. \end{aligned} \tag{A2}$$

In the first order of σ/v, we make the approximations

$$\int_{\pi/2}^{3\pi/2} \frac{d\varphi}{\left(-\frac{1}{\sigma}+\frac{\cos\varphi}{v}\right)^2} = \pi\sigma^2 - \frac{4\sigma^3}{v} \quad \text{and}$$

$$\int_{-\pi/2}^{\pi/2} \frac{d\varphi}{\left(-\frac{1}{\sigma}+\frac{\cos\varphi}{v}\right)^2} = \pi\sigma^2 + \frac{4\sigma^3}{v}. \tag{A3}$$

Due to $-b \ll \sigma_{EI}$ (19), the function g_2 is zero in the immediate vicinity of the point 0, so we can neglect $w_{EI}*g_2(0)$. We finally obtain

$$G_1(0) \approx \frac{2a_{EE}\sigma EE}{\pi v} - V_E. \tag{A4}$$

[1] B. Ermentrout, J. Comput. Neurosci. **5**, 191 (1998).
[2] P.A. Robinson, C.J. Rennie, and J.J. Wright, Phys. Rev. E **56**, 826 (1997).
[3] P.A. Robinson, J.J. Wright, and C.J. Rennie, Phys. Rev. E **57**, 4578 (1998).
[4] D. Golomb and B. Ermentrout, Proc. Natl. Acad. Sci. U.S.A. **96**, 13 480 (1999).
[5] D. Golomb and B. Ermentrout, Network Comput. Neural Syst. **11**, 221 (2000).
[6] M. Bazhenov *et al.*, J. Neurosci. **18**, 6444 (1998).
[7] M. Bazhenov *et al.*, J. Neurosci. **22**, 8691 (2002).
[8] A. Destexhe, D. Contreras, and M. Steriade, J. Neurosci. **19**, 4595 (1999)
[9] A. Destexhe, D. Contreras, and M. Steriade, Neurocomputing **38**, 555 (2001)
[10] D. Golomb, X.J. Wang, and J. Rinzel, J. Neurophysiol. **75**, 750 (1996).
[11] S.I. Amari, Biol. Cybern. **27**, 77 (1977).
[12] D.J. Pinto and G.B. Ermentrout, SIAM (Soc. Ind. Appl. Math.) J. Appl. Math. **62**, 206 (2001).
[13] D.J. Pinto and G.B. Ermentrout, SIAM (Soc. Ind. Appl. Math.) J. Appl. Math. **62**, 226 (2001).
[14] D. Golomb and G.B. Ermentrout, Phys. Rev. Lett. **86**, 4179 (2001).
[15] D. Golomb and G.B. Ermentrout, Phys. Rev. E **65**, 061911 (2002).
[16] H.R. Wilson and J.D. Cowan, Kybernetik **13**, 55 (1973).
[17] P.C. Bressloff, Physica D **155**, 83 (2001)
[18] D. Fender and B. Julesz, J. Opt. Soc. Am. **57**, 819 (1967).